

University of Massachusetts Amherst

From the Selected Works of Alfred Crosby

2006

Insight into the Periodicity of Schallamach Waves in Soft Material Friction

Charles J. Rand

Alfred Crosby, *University of Massachusetts - Amherst*



Available at: https://works.bepress.com/alfred_crosby/23/

Insight into the periodicity of Schallamach waves in soft material friction

Charles J. Rand and Alfred J. Crosby

Citation: *Applied Physics Letters* **89**, 261907 (2006); doi: 10.1063/1.2408640

View online: <http://dx.doi.org/10.1063/1.2408640>

View Table of Contents: <http://scitation.aip.org/content/aip/journal/apl/89/26?ver=pdfcov>

Published by the [AIP Publishing](#)

Advertisement:



Goodfellow

metals • ceramics • polymers
composites • compounds • glasses

Save 5% • Buy online
70,000 products • Fast shipping

Insight into the periodicity of Schallamach waves in soft material friction

Charles J. Rand and Alfred J. Crosby^{a)}

Department of Polymer Science and Engineering, University of Massachusetts, Amherst, Massachusetts 01003

(Received 27 July 2006; accepted 10 November 2006; published online 27 December 2006)

A dominant mechanism in friction of soft material interfaces is the onset and propagation of Schallamach waves. Schallamach waves are “tunnels” of air that provide relative displacement between the slider and the substrate rather than the instantaneous interfacial failure involved with stick-slip. Here, through model experiments and analysis, the authors present a fundamental relationship between the periodicity of Schallamach waves (λ) and the ratio of interfacial adhesion (\mathcal{G}_c) over complex elastic modulus (E^*). This deconvolution of bulk and interfacial contributions to the friction of soft materials leads to interesting predictions that will impact material design for a wide range of applications. © 2006 American Institute of Physics. [DOI: 10.1063/1.2408640]

From the design of biomaterials to the interpretation of nanoscale characterization of polymer interfaces, understanding the fundamentals of Schallamach waves¹ serves a critical purpose for a wide range of applications. By imaging a sliding interface, Schallamach¹ found that under certain conditions the frictional response of a rigid slider on a soft elastomer could proceed by means other than true sliding or stick-slip. Schallamach waves are surface instabilities that provide displacement between a slider and a substrate. The instability is argued by Barquins and Courtel² to be viscoelastic in nature, while Best *et al.*³ argue that it is purely elastic. Further work by Barquins and Roberts⁴ has given insight into the effect of testing geometry (i.e., load and radius of curvature) on the transition to Schallamach wave formation. Roberts and Jackson⁵ and Briggs and Briscoe⁶ have published fundamental energy balances for Schallamach waves relating them to tangential stress and frictional force, respectively. Since Schallamach’s discovery, there have been many attempts to explain Schallamach waves, but there exists no general relationship between Schallamach wave features and interfacial material properties. Here, through model experiments and analysis, we present a fundamental relationship between the periodicity of Schallamach waves (λ) and the ratio of interfacial adhesion (\mathcal{G}_c) over complex elastic modulus (E^*).

Schallamach waves are “tunnels” of air that provide relative displacement between the slider and the substrate rather than the instantaneous interfacial failure involved with stick-slip. To form these structures, the adhesive forces at the interface are strong enough to pin the interface in the rear creating a zone of tension, while shearing the interface causes a zone of compression in front of the contact area (i.e., elastic material ahead of the contact area in the direction of travel) [Fig. 1(a)]. If a critical compressive stress is reached prior to slip or other material failure, the material ahead of the interface will buckle as described from the theory of Biot.⁷ Briggs and Briscoe⁸ described the stress required to buckle a surface in similar tangential loadings as a simple multiple of the shear modulus (G) of the elastomer. If the resistance to interfacial separation (adhesion energy) is greater than the energy put into compressing the buckle

(stored elastic energy), the buckle will eventually attach to the slider. After attachment, the buckle forms a wave that passes through the interface providing a displacement between the substrate and the slider. An exaggeration of this mechanism is shown in Fig. 1(a).

To study Schallamach waves, a rigid lens was brought into contact with a soft elastomeric substrate that was laterally translated by an automated stage. A polished fused silica hemisphere ($R=5$ mm) (ISP Optics) was used as the slider. Cross-linked poly(dimethyl siloxane) (PDMS) (Dow Corning’s Sylgard® 184) was used as the substrate. The ratio of cross-linker to prepolymer was used to change the relative values of E^* and \mathcal{G}_c . The sliding velocity (v) was held constant for a given experiment, but ranged from 4 to 500 $\mu\text{m/s}$ over the complete set of experiments. A custom setup was built to allow for lateral force measurements, while applying a constant normal force (~ 25 mN). The interfacial contact

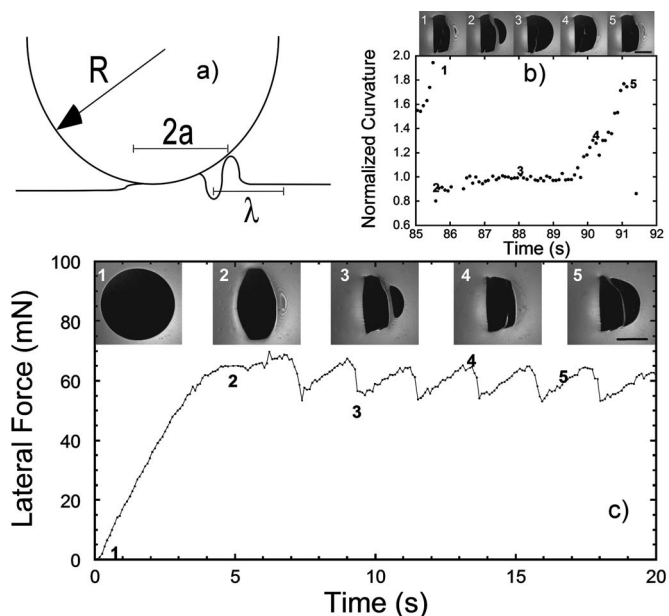


FIG. 1. (a) Schematic of Schallamach waves. (b) Normalized curvature of the contact area during one wave cycle, $R=5$ mm, $v=4.63$ $\mu\text{m/s}$, $E^*=0.9$ MPa at $\omega=0.3$ Hz. (c) Representative lateral force data with associated images of contact area, $R=5$ mm, $v=20.84$ $\mu\text{m/s}$, $E^*=0.9$ MPa at $\omega=0.3$ Hz [Scale bars in the last image of (b) and (c) represent 250 μm].

^{a)}Electronic mail: crosby@mail.pse.umass.edu

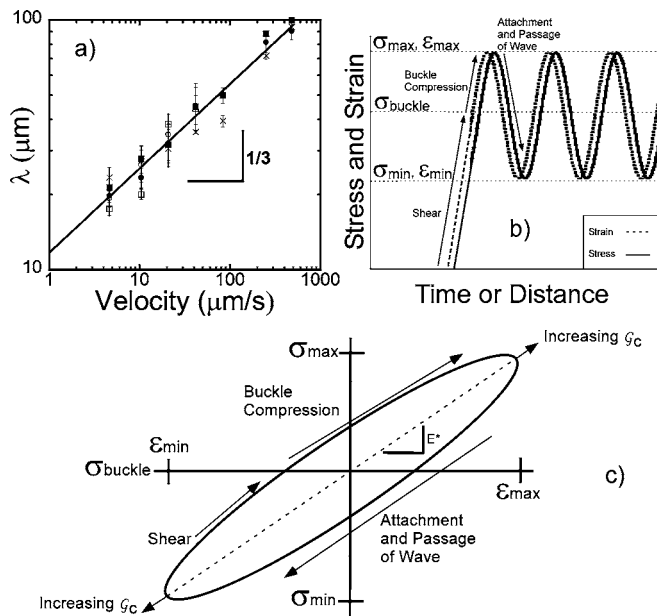


FIG. 2. (a) Buckle periodicity (λ) vs velocity. (b) Schematic of stress and strain vs time or distance. (c) Cyclical representation of a Schallamach wave [\circ — $E^* = 1.7$ MPa, \triangle — $E^* = 1.6$ MPa, \bullet — $E^* = 1.3$ MPa, \blacktriangle — $E^* = 0.9$ MPa, x — $E^* = 0.6$ MPa (E^* at $\omega = 0.3$ Hz), $R = 5$ mm].

area was imaged through the use of an inverted microscope. All data points presented are a statistical average of multiple runs on the same sample at the same conditions.

The contact area was imaged for all velocities and moduli tested. A typical evolution of the contact area is shown in Fig. 1(c). Upon shearing, the contact area quickly becomes noncircular and peels from the edges. Shearing, subsequent buckling, and buckle compression are associated with rise in the lateral force. Wave attachment and passage are associated with a decrease in the lateral force due to the addition of unsheared material to the interface along with the detachment of sheared material after the wave passes.

The curvature of the front of the contact area provides a clear indicator for the onset of Schallamach waves [Fig. 1(b)]. The curvature remains unchanged during the shear process before buckling occurs. At a critical force, buckling causes a sharp increase in the radius of curvature as material is peeled from the front portion of the slider and the front of the contact area becomes blunt. The buckle is compressed until attachment, which quickly brings the leading curvature back to its average prebuckle value.

The onset of a buckled surface in front of the sliding interface is a necessary but not sufficient condition for the formation of a Schallamach wave. Schallamach waves require the attachment of contact area after buckling, thus trapping a line of noncontact between the two regions of interface (Fig. 1). The distance between attachments is defined as the periodicity, λ , of the Schallamach waves. This defines the relative displacement between the slider and substrate achieved by each subsequent wave. Understanding the relationship between λ and material properties of the interface provides insight into the origin and underlying mechanism of Schallamach waves.

As Fig. 2(a) illustrates, for the material system tested, $\lambda \sim v^{1/3}$. The phenomena of increasing λ as a function of velocity can be directly explained using illustrations shown in Figs. 2(b) and 2(c). The process of Schallamach wave for-

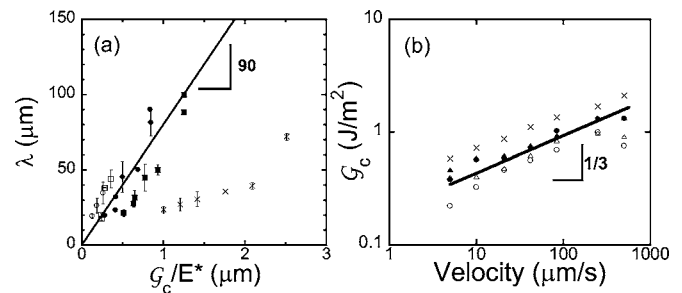


FIG. 3. (a) Buckle periodicity (λ) vs G_c over E^* . (b) G_c (mode I) vs velocity [\circ — $E^* = 1.7$ MPa, \triangle — $E^* = 1.6$ MPa, \bullet — $E^* = 1.3$ MPa, \blacktriangle — $E^* = 0.9$ MPa, x — $E^* = 0.6$ MPa (E^* at $\omega = 0.3$ Hz), $R = 5$ mm].

mation, attachment, and passage can be considered in terms of the stress and strain at the leading edge of the slider. During the initial translation of the slider, a compressive stress continuously increases until buckling occurs at a critical stress. Following buckling, the stress continues to rise as the buckle is compressed. After compression, the buckle attaches and passes through the interface formed between the slider and the substrate. This wave passing provides relief in stress and strain shown in Fig. 2(b) and is coincident with the addition of unsheared compressed material to the interface. The process repeats as sliding proceeds, thus establishing a periodic variation in the shear stress and strain at the leading edge. We can plot the periodic stress versus strain [Fig. 2(c)]. This schematic plot indicates the magnitude of energy loss in the Schallamach wave process by the hysteresis loop, and it provides insight into the role of G_c and E^* in controlling λ .

In terms of strain (ϵ), $\lambda \sim (\Delta\epsilon)(2a)$, where a is half the maximum contact width and $\Delta\epsilon = \epsilon_{\max} - \epsilon_{\min}$ for the leading edge during sliding. ϵ_{\min} is nearly zero for the freshly attached interface after wave passage, and $\epsilon_{\max} = \epsilon_{\text{buckle}} + (\epsilon_{\text{peel}} - \epsilon_{\text{buckle}}) \sim \sigma_{\text{peel}}/E^*$. Traditionally, the interfacial material property related to frictional mechanisms is G_c under mode II failure. For Schallamach waves, the primary mode of interfacial failure is mode I. This change in failure mode is due to a peeling moment dictated by the geometry of the buckled surface [Fig. 1(a)]. To pass a wave across the interface, the applied energy release rate (\mathcal{G}) at the leading edge of the wave must exceed or equal G_c for the material interface. Therefore, with the relation of λ to ϵ_{\max} and a general definition of peel energy release rate, $\lambda = (\beta)(G_c/E^*)$, where β is a geometrically defined constant.

Accordingly, λ is related to the balance of G_c and E^* [Fig. 3(a)]. This ratio defines a material length scale, whose velocity dependence dictates the velocity dependence of λ . This relationship clearly demonstrates that the velocity-dependent nature of Schallamach waves is not independently related to the bulk viscoelastic properties (E^*) or the velocity dependent interfacial properties (G_c), but rather the velocity dependence of the ratio G_c/E^* .

For many materials the velocity dependence of G_c or E^* may dominate the process. For our materials, E^* is essentially velocity or frequency independent, as measured by dynamic mechanical analysis, but G_c is dependent upon velocity [Fig. 3(b)]. G_c was measured using contact adhesion tests based on the theory of Johnson *et al.*⁹ This velocity dependence of G_c , for PDMS-PDMS and PDMS-glass interfaces, has been reported previously by many researchers and is largely related to the rate of bond dissociation.¹⁰ Therefore,

for this material interface, the velocity dependence of λ is not related to the bulk viscoelasticity, but rather to the frequency dependence of the interfacial strength.

The relationship between λ and \mathcal{G}_c/E^* in Fig. 3(a) works well except for the softest material. In this material [represented as X in Fig. 3(a)], the waves do not completely pass through the interface. They collapse during passage. This collapse indicates indirectly that mode I fracture geometry changes to mixed mode fracture for this material. Therefore, our \mathcal{G}_c/E^* scaling for Schallamach waves, which maintain mode I fracture during passage, will not hold for this material.

The deconvolution of the interfacial and bulk contributions to Schallamach waves suggests interesting predictions. If materials are appropriately designed, the velocity dependence of \mathcal{G}_c could be tuned to relate to the velocity dependence of E^* , such that the friction of a viscoelastic material would be independent of velocity. Second, the relationship of λ to \mathcal{G}_c/E^* suggests that the periodicity of Schallamach waves will quickly approach nanometer length scales for more rigid materials. Direct observation of these waves will be challenging, but their impact on wear mechanisms would be extremely relevant to the design of materials.

In this study, experiments to understand the fundamentals of Schallamach waves were conducted. It was found that the leading edge curvature provides a better understanding of the distinct events involved with Schallamach wave forma-

tion, attachment, and passage. The balance of interfacial and bulk contributions, as described by the material length scale \mathcal{G}_c/E^* , was related to the periodicity (λ) of Schallamach waves. This deconvolution was introduced through the analysis of Schallamach waves in terms of the stress-strain cycles at the leading edge of the interface. This insight leads to interesting predictions that will impact material design for the wide range of applications where Schallamach waves are observed or anticipated.

The work is supported by the NSF Career Award No. DMR-0349078, NSF-MRSEC at the University of Massachusetts, and Army Research Laboratory Center of Excellence at the University of Massachusetts.

¹A. Schallamach, *Wear* **17**, 301 (1971).

²M. Barquins and R. Courtel, *Wear* **32**, 133 (1975).

³B. Best, P. Meijers, and A. R. Savkoor, *Wear* **65**, 385 (1981).

⁴M. Barquins and A. D. Roberts, *J. Phys. D* **19**, 547 (1986).

⁵A. D. Roberts and S. A. Jackson, *Nature (London)* **257**, 119 (1975).

⁶G. A. D. Briggs and B. J. Briscoe, *Nature (London)* **262**, 381 (1976).

⁷M. A. Biot, *Proc. R. Soc. London, Ser. A* **273**, 329 (1963).

⁸G. A. D. Briggs and B. J. Briscoe, *Philos. Mag. A* **38**, 387 (1978).

⁹K. L. Johnson, K. Kendall, and A. D. Roberts, *Proc. R. Soc. London, Ser. A* **324**, 301 (1971); K. R. Shull, *Mater. Sci. Eng., R.* **36**, 1 (2002).

¹⁰M. K. Chaudhury, *J. Phys. Chem. B* **103**, 6562 (1999); S. Perutz, E. J. Kramer, J. Baney, C. Y. Hui, and C. Cohen, *J. Polym. Sci., Part B: Polym. Phys.* **36**, 2129 (1998)